RSC Advances

PAPER

View Article Online
View Journal | View Issue

Cite this: *RSC Adv.*, 2022, **12**, 728

Phthalide-containing poly(ether-imide)s based thermal rearrangement membranes for gas separation application

Lei He,[a] Yunhua Lu,*[a] Guoyong Xiao,[a] Mengjie Hou,[b] Haijun Chi[a] and Tonghua Wang*[b]

The diamine monomer 3,3-bis[4-(3-hydroxy-4-amino-phenoxy)phenyl]phthalide (BHAPPP) was firstly synthesized by the nucleophilic substitution of 5-fluoro-2-nitrophenol and phenolphthalein, followed by a reduction reaction. A series of phthalide-containing poly(ether imide)s (PEI) were then prepared through the polycondensation of BHAPPP with six kinds of dianhydrides, including 4,4′-(hexafluoroisopropylidene)diphthalic anhydride (6FDA), 3,3′,4,4′-benzophenone tetracarboxylic dianhydride (BTDA), 3,3′,4,4′-biphenyl tetracarboxylic dianhydride (BPDA), 4,4′-oxydiphthalic dianhydride (ODPA), 1,2,3,4-cyclobutane tetracarboxylic dianhydride (CBDA) and pyromellitic dianhydride (PMDA), as well as thermal imidization. After further thermal treatment, the corresponding thermal rearrangement (TR) membranes were obtained. Due to the existence of the phthalide lactone ring, the PEIs probably underwent TR and crosslinking simultaneously. With the increase of thermal treatment temperature, the mechanical properties of the TR membranes dramatically decreased, but the gas separation properties obviously increased. When the PEIs were treated at 450 °C for 1 h, the CO_2, H_2, O_2, N_2 and CH_4 permeability of TR(BHAPPP-6FDA) reached 258.5, 190.5, 38.35, 4.25 and 2.15 Barrers, respectively. Meanwhile, the CO_2/CH_4 selectivity of 120.2 sharply exceeded the 2008 Robeson limit, and O_2/N_2 selectivity was 9.02, close to the 2015 upper limit. Therefore, the TR membranes derived from phthalide-containing PEIs exhibit superior gas separation performance, andare expected to be applied in the field of gas separation.

Received 19th September 2021
Accepted 18th December 2021

DOI: 10.1039/d1ra07013d

rsc.li/rsc-advances

1. Introduction

Gas membrane separation technology is a kind of new and efficient separation technology, which has attracted wide attention because of the advantages of being environment friendly, and having a low energy consumption and easy operation.[1,2] The separation membrane is the key material of this technology, mainly involving polymeric membrane and carbon membrane. Up to now, polymeric membrane has been mainly applied as a commercial separation membrane material, like silicon rubber, polyimide (PI) and polysulfone.[3–7] Moreover, polymer membrane exhibits a "trade-off" relationship between gas permeability and selectivity, which greatly limits its practical application.[8–11] Among polymer materials, PI is favored by engineers and researchers due to its excellent thermal stability, mechanical properties and chemical solvent resistance.[12–14] However, the low gas permeability of dense PI membrane commonly leads to a decrease of separation efficiency.

It is well known that gas permeability of polymer membranes is closely related to the free volume, which provides narrow tunnels for the transport of gas molecules. In order to increase the free volume of PI, some feasible methods have been proposed, including the introduction of bulky Cardo structure, triptycene group, large volume substituent and contorted linkage.[15–20] For instance, the introduction of bulky Cardo group can increase the interchain distance, reduce the interaction between molecular chains, and form more free volume, which is conducive to the transportation of gas molecules. Meanwhile, rigid macromolecular chains are always preferred for gas separation membranes to maintain high gas selectivity. As a result, the gas separation properties of PI membrane materials have been dramatically improved by these efforts.[21–28]

In recent years, thermal rearrangement (TR) polymers have been developed and investigated by researchers in the field of membrane separation.[29–34] Due to the transition from imide ring to benzoxazole structure, hydroxyl-containing polyimide (HPI) is transformed into polybenzoxazole (PBO), and a large amount of small molecule gas CO_2 is released.[35–41] TR polymers exhibit excellent gas permeability and moderate selectivity because of unique "hourglass" micropore structure, which have become a new generation of gas separation membrane

[a]School of Chemical Engineering, University of Science and Technology Liaoning, Anshan, Liaoning, 114051, P. R. China. E-mail: lee.lyh@163.com
[b]School of Chemical Engineering, Dalian University of Technology, Dalian, Liaoning, 116024, P. R. China. E-mail: wangth@dlut.edu.cn

materials.[42] The gas separation process of TR polymer is mainly followed by the solution-diffusion mechanism, accompanied by the sieving mechanism due to the existence of pore structures. According to the literatures,[29–44] the rearrangement reaction and gas separation performance of TR polymers are mostly affected by many factors, such as chemical structure, glass transition temperature (T_g), thermal treatment atmosphere, time and temperature. For example, the HPI containing flexible linkage is easy to rearrange at a relatively low temperature because of better motion ability of chain segment, but the increase of gas permeability is not very significant. On the contrary, the HPI with rigid backbone needs higher rearrangement temperature to conduct the structural transformation, resulting in high gas permeability.

It is well known that the crosslinking could limit the movement of macromolecular chains and even release small molecule gas CO_2, which is helpful to improve the gas permeability, selectivity and plasticizing resistance of membrane materials.[45–51] For polyimide, 3,5-diaminobenzoic acid is a common crosslinking monomer to form crosslinking structure after decarboxylation reaction.[52] Besides, it is recently reported that the gas separation performance of polymer membranes has been improved by the crosslinking of phthalide ring.[47–50] For instance, our cooperative research group found that the poly aryl ether ketone (PEK-C) membrane with phthalide groups was thermally crosslinked by the decomposition of the lactone rings and further decarboxylation in N_2 atmosphere.[47] The gas separation and anti-plasticization properties of PEK-C membrane were significantly enhanced due to the enlargement of the interchain distance and formation of free volume cavity. Especially, the permeability of CO_2 was 110 times higher than that of the original PEK-C membrane. Moreover, Caili Zhang *et al.* reported that the thermal oxidation crosslinking in air for PI membranes containing phthalide groups took place at a relatively lower temperature than the carboxylic acid containing polyimides, which greatly enhanced the gas separation properties.[48] Thereby, phthalide group, as a kind of Cardo structure, has large steric hindrance and asymmetric structure, which is beneficial to decrease the packing density and enhance the free volume of polymers. In addition, after certain heat treatment, phthalide lactone ring could be broken, followed by the formation of crosslinked structures.[47–50] Therefore, the phthalide-containing PIs are attracting the attention of researchers in the field of membrane materials.

In this work, the diamine monomer containing phthalide group and ether linkage, 3,3-bis[4-(3-hydroxy-4-amino-phenoxy) phenyl]phthalide (BHAPPP) was firstly synthesized by the nucleophilic substitution of 5-fluoro-2-nitrophenol and phenolphthalein, followed by reduction reaction. Then, a series of phthalide-containing poly(ether imide)s (PEI) were prepared through the solution-polymerization of BHAPPP with six kinds of dianhydrides, followed by thermal imidization. After further thermal treatment, the corresponding TR membranes were obtained, accompanied with crosslinking reaction. The effects of chemical structure of dianhydrides and thermal treatment temperature on the structures and properties of the final membrane materials were studied. Due to the introduction of phthalide group, these TR membranes exhibited excellent gas permeabilities, coupled with proper selectivities, which are expected to be used in the field of gas separation.

2. Experimental

2.1 Materials

5-Fluoro-2-nitrophenol and phenolphthalein were purchased from Shanghai Haohong Biomedical Technology Co., Ltd. (China). Pyromellitic dianhydride (PMDA) was bought from Sinopharm Chemical Reagent Co., Ltd. (China). 1,2,3,4-Cyclobutane tetracarboxylic dianhydride (CBDA) was obtained from Liaoning Oxilan Huahui New Material Co., Ltd. (China). 4,4′-(Hexafluoroisopropylidene)diphthalic anhydride (6FDA), 3,3′,4,4′-benzophenone tetracarboxylic dianhydride (BTDA), 3,3′,4,4′-biphenyl tetracarboxylic diandhydride (BPDA) and 4,4-oxydiphthalic dianhydride (ODPA) were purchased from Tianjin Chinatech Chemical Co., Ltd. (China). Pd/C (10% Pd), hydrazine hydrate, potassium carbonate (K_2CO_3), ethanol, *N*,*N*-dimethylformamide (DMF) and *N*,*N*-dimethylacetamide (DMAc) were obtained from Sinopharm Chemical Reagent Co., Ltd. (China). The six anhydrides need to be fully dried at 180 °C for 24 h before use, and other chemicals were directly used.

2.2 Synthesis of diamine monomer

(a) Synthesis of 3,3-bis[4-(3-hydroxy-4-nitrophenoxy) phenyl]phthalide (BHNPPP). The preparation process is shown in Scheme 1. 5.000 g (15.7 mmol) of phenolphthalide, 4.936 g (31.4 mmol) of 5-fluoro-2-nitrophenol and 4.338 g (31.4 mmol) of K_2CO_3 were added to a 100 mL two-neck round-bottom flask with 25 mL DMF. Under stirring, the mixture was heated to 150 °C for 12 h. After cooling to room temperature, some ice water was poured into the mixed solution to produce the yellow precipitates. The crude products were washed with deionized water for several times and dried in a vacuum oven at 80 °C for 24 h. The relative purity of dinitro compound BHNPPP was 98% (HPLC), and the yield was about 75%. Melting point: 320 °C (DSC). ^{1}H NMR (500 MHz, DMSO) δ: 11.14 (s, 2H), 7.99 (d, 1H), 7.98 (d, J = 2.9 Hz, 1H), 7.92 (t, J = 7.2 Hz, 1H), 7.73 (t, J = 7.5 Hz, 1H), 7.46 (d, J = 8.8 Hz, 4H), 7.24 (d, J = 8.8 Hz, 4H), 6.61 (d, J = 2.6 Hz, 2H), 6.58 (t, J = 1.9 Hz, 4H). FTIR: 3280 cm^{-1} (O–H stretching vibration), 1585–1324 cm^{-1} (N–O symmetric stretching vibration) 1251–1218 cm^{-1} (=C–O stretching vibration).[32,35,48]

(b) Synthesis of 3,3-bis[4-(3-hydroxyl-4-aminophenoxy) phenyl]phthalide (BHAPPP). 5.000 g (9.3 mmol) BHNPPP and 0.250 g (7.0 mmol) Pd/C were placed into a 100 mL two-neck round-bottom flask with 30 mL of ethanol as solvent. In the reflux state, 20 mL hydrazine hydrate was slowly added dropwise to the solution. After 12 h of continuous reaction, the Pd/C was removed by hot filtration, and the residual filtrate was poured into a large amount of deionized water. There were a lot of white products, which were filtrated, washed with deionized water and dried in a vacuum oven at 60 °C for 24 h. The relative purity of diamine BHAPPP was 98% (HPLC), and the productivity was about 75%. Melting point: 120 °C (DSC). ^{1}H NMR (500

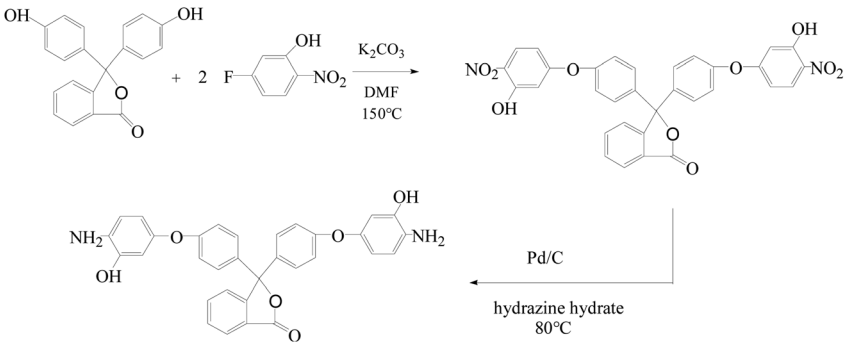

Scheme 1 Synthetic route of BHNPPP and BHAPPP.

MHz, DMSO) δ: 9.25 (s, 2H), 7.93 (d, $J = 7.6$ Hz, 1H), 7.87–7.82 (t, 2H), 7.67 (t, $J = 5.5$ Hz, 1H), 7.23 (d, $J = 8.9$ Hz, 4H), 6.87 (d, $J = 8.9$ Hz, 4H), 6.58 (d, $J = 8.4$ Hz, 2H), 6.38 (d, $J = 2.6$ Hz, 2H), 6.30 (dd, $J = 8.4$, 2.6 Hz, 2H), 4.45 (s, 4H). FTIR: 3378–3308 cm^{-1} (N–H stretching vibration), 3171 cm^{-1} (O–H stretching vibration), 1256–1219 cm^{-1} (═C–O stretching vibration).[32,35,48]

2.3 Preparation of PEI and TR membranes

The PEI membranes were prepared according to the thermal imidization method (Scheme 2). First, the diamine BHAPPP (4.0 mmol, 2.218 g) and 22.63 mL DMAc were added to a 100 mL two-neck round-bottom flask equipped with a mechanical stirrer. After stirring for 30 min, the equimolar dianhydride 6FDA was introduced and stirred continuously for 12 h. Then, the polyamic acid (PAA) solution with a concentration of 15 wt% was synthesized, which was evenly coated on a clean glass substrate. After the step-by-step heating treatment, including 50 °C for 2 h, 80 °C for 1 h, 150 °C for 1 h, and 250 °C for 0.5 h, the PEI membrane was obtained and named as PEI(BHAPPP-6FDA). Next, the membrane was further thermally treated in a tube furnace at a heating rate of 3 °C min^{-1} and a N_2 flow rate of 200 mL min^{-1}, and the final temperature was set at 450 °C and kept for 1 h. The obtained membrane was called as TR(BHAPPP-6FDA). Finally, other PEI and TR membranes were also prepared according to this process.

2.4 Characterization

The chemical structures of the compounds and polymer membranes were identified by a Is10 Fourier transform infrared spectrometer (FT-IR) instrument (Nicolet, USA) in the range of 4000 to 500 cm^{-1}. The chemical shifts of BHNPPP and BHAPPP were detected by an Agilent-500 Nuclear magnetic resonance (NMR) spectrometers with deuterated DMSO as the solvent (Agilent, USA). After platinum spraying treatment, the fracture surface morphology of TR membrane was observed by an Apreo 2S Field emission scanning electron microscope (FE-SEM) (Thermo Fisher Scientific, US). The specific surface area and pore size were determined by a nitrogen adsorption–desorption test on Quantachrome Autosorb IQ-XR analyzer (US) at 77 K. The microstructures of the polymers were confirmed by a D8 ADVANCE X-ray diffractometer (XRD) (Bruker, German) with a scanning range $2\theta = 10$–70°. According to Bragg equation ($2d \sin\theta = n\lambda$, $\lambda = 1.54$ Å), the d-spacing values of polymer membranes were calculated. The mechanical properties, including tensile strength, Young's modules and broken elongation, were measured by a HY0350 Universal material tensile testing machine (Shanghai Hengyi Precision Instrument Co. Ltd., China) with 5 cm of tested gauge length and 10 mm min^{-1} of tensile rate. The melting point of compounds and glass transition temperature (T_g) of polymers were measured by DSC 4000 Differential scanning calorimetry (DSC) analyzer (PerkinElemer, USA) and DMA 8000 Dynamic thermomechanical analyzer (DTMA) (PerkinElemer, USA) in nitrogen atmosphere from 50 to 400 °C at a heating rate of 20 °C min^{-1} and 10 °C min^{-1}, respectively. The STA 449F3 Thermogravimetric mass spectrometry (TG-MS) (Netzsch, Germany) was employed to test the thermal properties of PEI samples from room temperature to 900 °C at a heating rate of 10 °C min^{-1} under 50 mL min^{-1} of N_2 flow. The chemical elements on the surface of membrane sample were characterized by an ESCALAB250Xi X-ray photoelectron spectroscopy (XPS) instrument (Thermo Fisher Scientific, USA).

The gas permeabilities of the membranes were measured by a lab self-made permeation cell with constant-volume and variable-pressure method using high-purity gases at 30 °C and 0.01 MPa (0.1 atm). The thicknesses of these membranes were about 55 ± 10 μm. Under the same test conditions, each membrane material was cut into 1.5 cm × 1.5 cm. More than 3 samples were tested to obtain the average value, and the measurement accuracy was about ±10%. During the test, the membrane was unsupported. The gas permeability and selectivity were calculated according to the following formula:

$$P_i = \frac{F/S}{\Delta P/L} \quad (1)$$

$$\alpha_{A/B} = \frac{P_A}{P_B} \quad (2)$$

where P_i represents the permeability to i gas (Barrer, 1 Barrer = 1×10^{-10} cm^3(STP) cm cm^{-2} s^{-1} cm Hg^{-1}), F means the gas volume flow rate, L is the thickness of the membranes, S represents the effective area of gas passing through the membranes and ΔP is the pressure differential between the gas

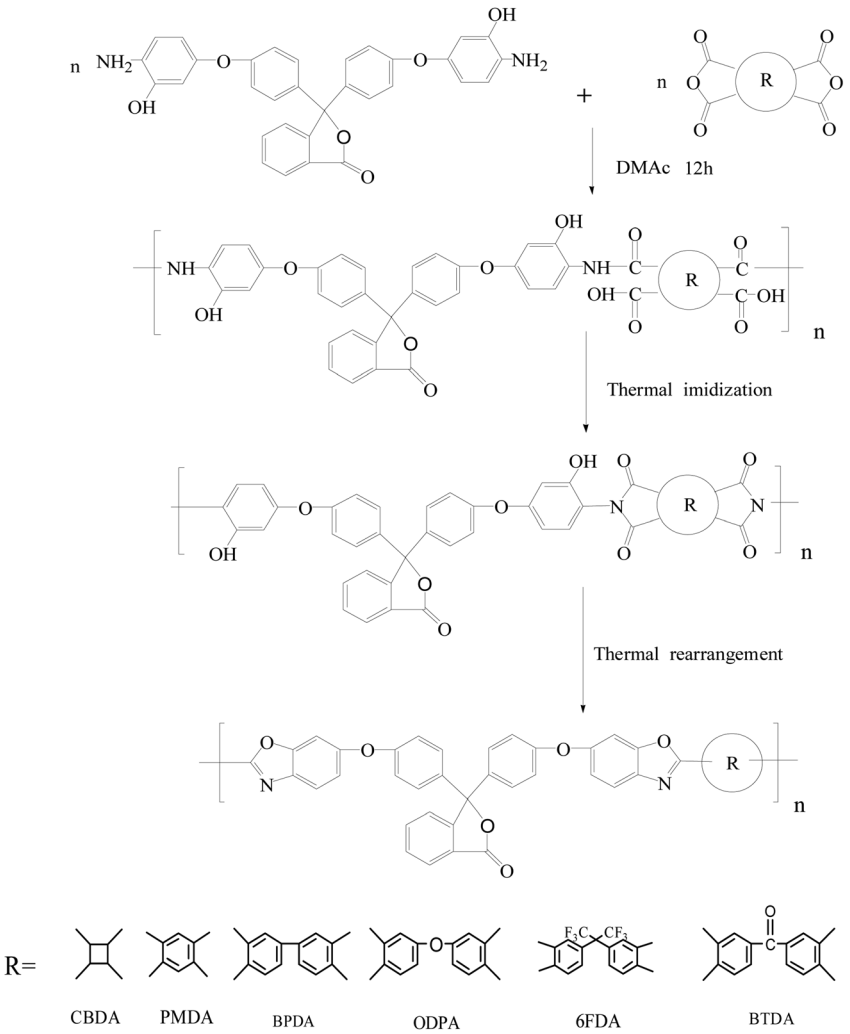

Scheme 2 Preparation of PEI and TR membranes.

through the membranes. P_A and P_B are the permeability of gas A and B, and $\alpha_{A/B}$ represents the ideal selectivity of gas A to B.

3. Results and discussion

3.1 Chemical structures of PEI and TR membranes

The change of chemical structures from PEI to TR polymers was confirmed by FTIR in Fig. 1. For the PEI polymers (Fig. 1(a)), the asymmetric and symmetrical stretching vibration absorption peaks of C=O in the imide ring appear at 1779 and 1720 cm^{-1}, and the characteristic peak at 1381 cm^{-1} is assigned to the C–N bond of imide ring, which indicate that the imide ring structures have been mostly formed. After the thermal treatment at 450 °C for 1 h, these special peaks for imide ring are obviously weakened, which are probably caused by the thermal rearrangement from HPI to PBO (Fig. 1(b)). At the same time, the absorption peaks of –N=C–O at around 1054 and 1546 cm^{-1}, indicating that the rearrangement reaction is induced.[38]

The images of six PEI and TR(BHAPPP-6FDA) membranes are shown in Fig. 2. It can be seen that six kinds of PEI membranes show different colors and good film-formation, in which PEI(BHAPPP-PMDA) and PEI(BHAPPP-BTDA) exhibit dark yellow due to the absorption of light by electron transfer complex (CTC) formed between dianhydrides and diamines.[53] The phthalide groups with bulky and non-coplanar structure increase the distance between molecular chains, destroy the regularity of macromolecular chains and decrease the interaction between molecular chains, which are benefit to improve the transparency of the PEI membranes.[47,48] Moreover, these PEI membranes show excellent film-formation due to the presence of ether linkage, and the final TR membranes still show better flexibility to meet subsequent measurement.

The element composition and electronic states on the surface of TR(BHAPPP-6FDA) were characterized by XPS in Fig. 3, from which four main elements of C, N, O and F are clearly observed at 285, 399, 531 and 687 eV. The C, O and N curves were further fitted to analyze the chemical structure. In Fig. 3(b), there are six characteristic fitting peaks, including C–C (284.7 eV), C–N (285.5 eV), C–O (286.3 eV), C=N (287.2 eV) and C=O (288.3 eV), which show that the PEI has partly undergone thermal rearrangement from PEI to PBO. In the O1s fitting curves (Fig. 3(c)), the two peaks at 288.3 and 285.5 eV represent

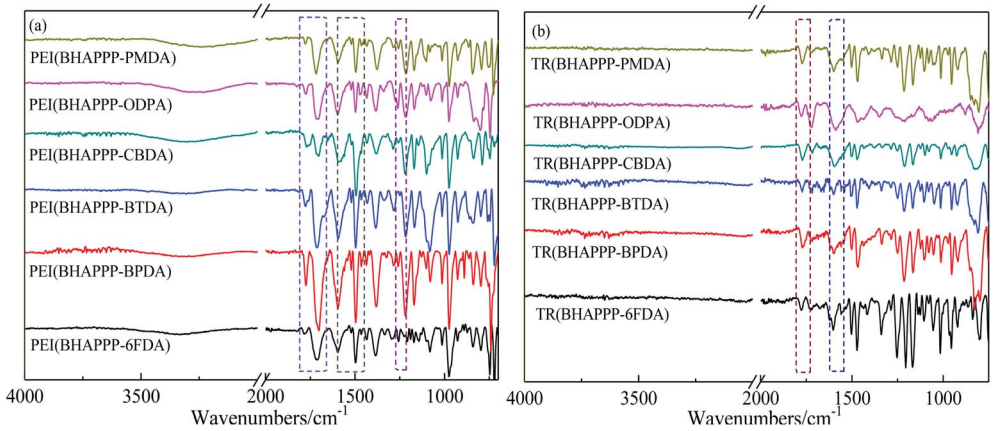

Fig. 1 FTIR spectra (a) PEI membranes, (b) TR membranes.

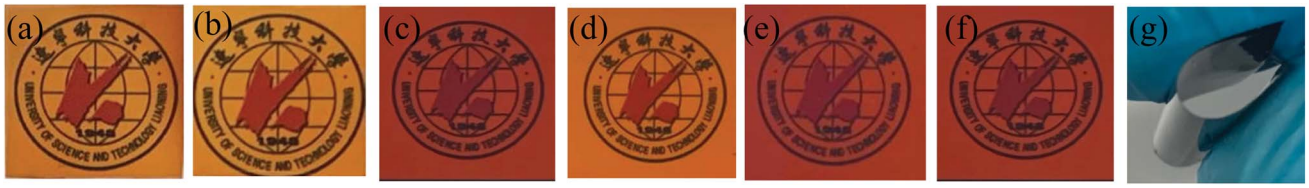

Fig. 2 Images of PEI and TR membranes (a) PEI(BHAPPP-6FDA), (b) PEI(BHAPPP-BPDA), (c) PEI(BHAPPP-PMDA), (d) PEI(BHAPPP-ODPA), (e) PEI(BHAPPP-BTDA), (f) PEI(BHAPPP-CBDA), (g) TR(BHAPPP-6FDA).

C═O and C–O, respectively. By calculating the peak area of –N< (400.2 eV) corresponding to imide ring and C═N– (399.1 eV) assigned to benzoxazole structure in Fig. 3(d), the conversion degree of thermal rearrangement could be roughly estimated to be 53.45%, indicating a partial conversion under the condition of 450 °C for 1 h.

3.2 Thermal properties of PEI and TR membranes

It was reported by Caili Zhang *et al.* that the phthalide lactone ring of 6FDA-MPP synthesized by chemical imidization began to be decomposed and formed free radicals during the TGA test of 225–375 °C in N_2. However, Ruisong Xu *et al.* reported that the lactone rings in the phthalide Cardo moieties of PEK-C decomposed and released CO_2 along with forming phenyl and methine free radicals during the thermal treatment of 400–500 °C in N_2. Finally, two adjacent phenyl radicals are most likely to combine to form a biphenyl crosslinking structure.[47] Furthermore, the thermal stability of aromatic polymers containing phthalide structures is generally excellent, with a high initial thermal decomposition temperature above 400 °C. We infer that the weight loss around 300 °C is more likely to be caused by incomplete imidization. Thus, the TGA-MS curves of PEI(BHAPPP-6FDA) tested in N_2 and air were used to estimate the TR and crosslinking process, as shown in Fig. 4.

As can be seen from Fig. 4(a), there are three main weightlessness peaks under the condition of N_2 and air. The first small weight loss around 300 °C is probably caused by the further imidization reaction. Because the PEI membranes were finally treated at 250 °C for 30 min, the residual PAA continued to be closed ring during the test. The second peak around 400 °C is mainly attributed to the thermal rearrangement reaction, which may be accompanied by the decomposition of phthalide groups to form phenyl radical and methyl radical, leading to weight loss.[48,51,55] The HPI could undergo thermal rearrangement to from PBO, coupled with the release of CO_2 gas. This result is consistent with some studies on thermally rearranged polymers.[56–58] Moreover, the phthalide lactone ring may be opened and remove CO_2 to form a crosslinked structure.[50,54] The third peak of significant weightlessness about 520 °C is induced by the thermal decomposition of the main chain of polyimides.[33,38] In N_2 and air atmospheres, the degree of thermal rearrangement and decomposition reactions is obviously different. It is clear that the thermal rearrangement reaction is easier to be carried out in nitrogen atmosphere. Besides, according to the MS = 44(CO_2) curves in Fig. 4(b), the CO_2 is mainly released in the two temperature ranges, including around 400 °C assigned to the thermal rearrangement and possible decomposition of phthalide group as well as after 500 °C caused by the pyrolysis of polymer backbone. Considering the ability and type of TR and decomposition, the rearrangement reaction might be earlier than the thermal decomposition of phthalide structures. Hence, the thermal treatment temperature was set around the reaction temperature in N_2.

In order to further study the thermal properties of the PEI samples, DSC and DMA measurements were conducted, and the corresponding results were given in Fig. 5 and Table 1. Generally, the T_g values of these PEIs are from 322 to 352 °C by DSC and from 325 to 378 °C by DTMA, which are higher than those of

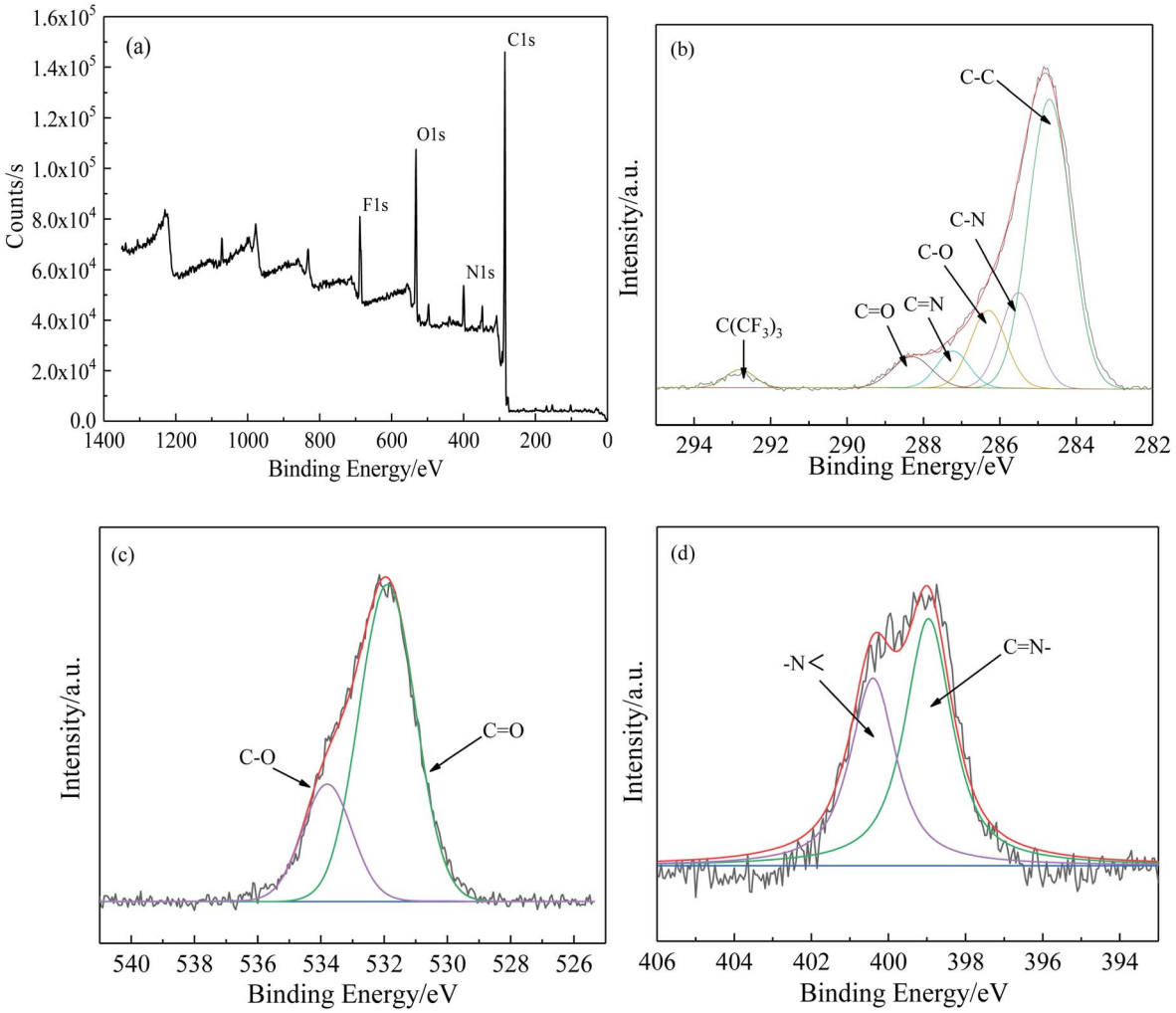

Fig. 3 XPS spectra of TR(BHAPPP-6FDA) (a) wide scan spectra, (b) fitting curves of C 1s, (c) fitting curves of O 1s, (d) fitting curves of N 1s.

the polyimide containing phthalide group without hydroxyl groups.[48,50] Due to the formation of hydrogen bond, the existence of hydroxyl groups could increase the interaction between the molecular chains and limit the movement of HPI segments, resulting in excellent thermal properties. As for the same diamine BHAPPP, the chemical structure of dianhydride directly affects the properties of PEIs. Comparatively speaking, the PEI(BHAPPP-ODPA) shows a lower T_g because of the flexibility of ether linkage. Meanwhile, the PEIs derived from rigid dianhydrides, such as PEI(BHAPPP-PMDA) and PEI(BHAPPP-

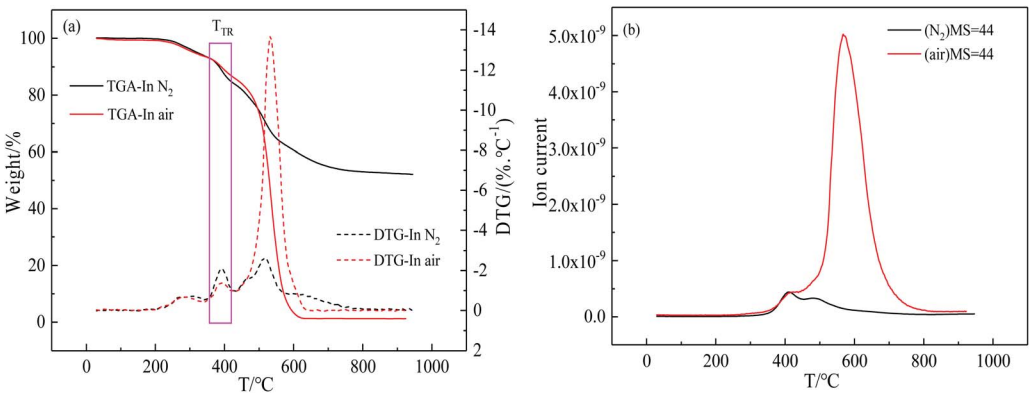

Fig. 4 TGA-MS curves of PEI(BHAPPP-6FDA) in N_2 and air (a) TGA curves, (b) MS = 44 curves.

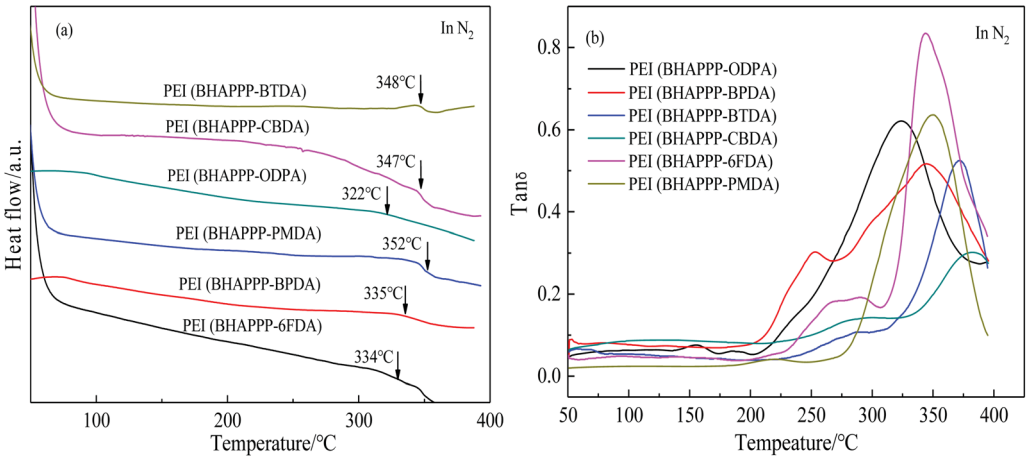

Fig. 5 (a) DSC curves of PEI membranes (b) tan δ–T curves of PEI membranes.

Table 1 Thermal and mechanical properties of PEI membranes

	T_g (°C)				
Samples	DTMA	DSC	Tensile strength (MPa)	Young's modulus (GPa)	Elongation at break (%)
PEI(BHAPPP-BPDA)	344	335	108.2 ± 3.0	4.1 ± 0.1	3.0 ± 0.2
PEI(BHAPPP-BTDA)	372	348	122.9 ± 2.0	3.7 ± 0.2	4.4 ± 0.1
PEI(BHAPPP-CBDA)	378	347	92.8 ± 3.0	5.1 ± 0.2	1.8 ± 0.2
PEI(BHAPPP-ODPA)	325	322	88.7 ± 2.0	4.4 ± 0.2	2.0 ± 0.2
PEI(BHAPPP-PMDA)	350	352	94.3 ± 2.0	4.5 ± 0.2	2.5 ± 0.2
PEI(BHAPPP-6FDA)	343	334	85.4 ± 2.0	3.3 ± 0.2	2.6 ± 0.1
PEI(BHAPPP-6FDA)-375	—	—	47.1 ± 2.0	2.5 ± 0.2	1.8 ± 0.1
PEI(BHAPPP-6FDA)-400	—	—	33.6 ± 2.0	2.1 ± 0.1	1.5 ± 0.2
PEI(BHAPPP-6FDA)-425	—	—	18.8 ± 1.0	2.6 ± 0.2	0.7 ± 0.1
PEI(BHAPPP-6FDA)-450	—	—	14.2 ± 1.0	2.2 ± 0.1	0.5 ± 0.1
PEI(BHAPPP-6FDA)-475	—	—	9.8 ± 1.0	1.3 ± 0.1	0.5 ± 0.1

CBDA), exhibit higher T_g values. Furthermore, the bulky phthalide group could increase the steric hindrance and hinder the movement of segments. Therefore, these phthalide-containing PEIs display excellent thermal properties.

3.3 Microstructure of PEI and TR membranes

The surface morphology of broken TR(BHAPPP-6FDA) membrane was observed by SEM, as shown in Fig. 6. It is clear that the surface is uniform and dense, without obvious defects. Furthermore, the curve of pore size distribution obtained from N_2 adsorption–desorption measurement is given in Fig. 7. The pore width is chiefly centered at 2–7 nm, and the specific surface area is 94.162 $m^2\ g^{-1}$. The introduction of micro/meso pores is desirable in the transport of gas molecules. Thus, the TR(BHAPPP-6FDA) polymer exhibits porous microstructure, which is expected to be applied as the gas separation membranes.

In order to further clarify the microstructural change of the polymer membranes, XRD measurement was carried out. As we know, the gas separation mechanism of polymer membranes is reasonably explained by solution-diffusion process, in which the free volume plays a very important role for gas transport.[14–16] Based on XRD results, the obtained d-spacing value could be used to realize the microstructure of membrane materials. A larger d-spacing value is often more conducive to the transport of gas molecules, resulting in a higher gas permeation flux.[15,16,28,59] The XRD curves of PEI and TR membranes are shown in Fig. 8. It is found from Fig. 8(a) that the PEI(BHAPPP-6FDA) exhibits a larger d-spacing about 0.54 nm, while other PEIs show d-spacing values around 0.43 nm. The introduction of bulky and non-coplanar hexafluoroisopropyl group in 6FDA could increase the distance and destroy the close stacking of macromolecular chain, resulting in the formation of high free volume.[14,15,38] The physical properties of these PEIs are recorded in Table 2, and the fractional free volume (FFV) is calculated according to the Bondi method, which is basically consistent with the d-spacing values. Cardo structure is conducive to increase the distance between molecular chains, and flexible ether bond is helpful to close the arrangement of molecular chains. Under the two effects, the dianhydride plays a more important role in the layer spacings. In Fig. 8(b), after thermal rearrangement at 450 °C for 1 h, the layer spacings of these TR membranes enhance with varying degrees, among which

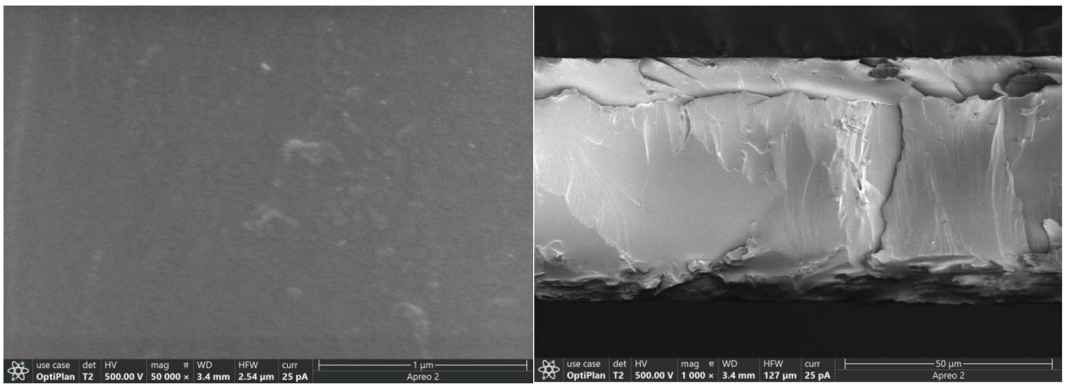

Fig. 6 FE-SEM images of fracture surface of TR(BHAPPP-6FDA).

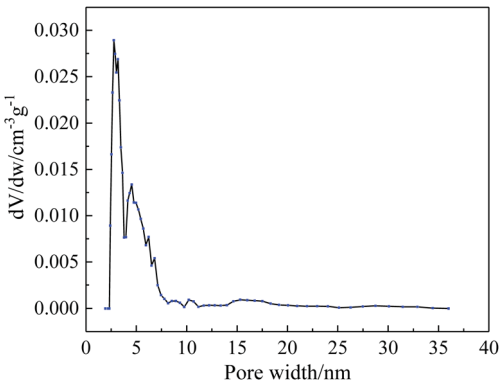

Fig. 7 Pore size distribution curve of TR(BHAPPP-6FDA) membrane.

TR(BHAPPP-6FDA) exhibits an obvious increase of *d*-spacing from 0.54 to 0.63 nm. The *d*-spacing is larger than that of other reported PI containing phthalide structure, such as TCM-450-1 h[47] and 6FDA-MPP-400,[48] which extremely contributes to the improvement of gas transmission. Hence, the TR membrane based on 6FDA is more suitable for gas separation membrane materials. The effect of thermal treatment temperature on the layer spacings of TR(BHAPPP-6FDA) membranes are investigated by the XRD curves in Fig. 8(c). With the increase of thermal treatment temperature, the interlayer spacing increases gradually, which is mainly due to the increasing conversion degree of rearrangement. Thus, the microstructure of TR membranes could be obviously affected by the thermally treated temperature.

3.4 Mechanical properties of PEI and TR membranes

Because gas separation membranes are often used in high temperature and high pressure environment, the mechanical properties of membrane materials are very important for its practical application. The stress–strain curves of PEI and TR(BHAPPP-6FDA) membranes are shown in Fig. 9, and the corresponding mechanical properties are listed in Table 1. The tensile strength, Young's modulus and elongation at break of PEI membranes are 85.4–122.9 MPa, 3.3–5.1 GPa and 1.8–4.4% respectively, indicating that they have excellent mechanical properties to undergo further thermal treatment. For these PEI membranes, the existence of flexible ether bond is helpful to improve the film-formation and mechanical properties. Among them, the PEI membranes derived from rigid dianhydrides PMDA, BPDA and CBDA exhibit higher tensile strength and modulus. The PEI derived from dianhydride BTDA exhibits the highest tensile strength, which may be ascribed to the oxidative crosslinking and hydrogen bonding due to the existence C=O. After thermal treatment, the mechanical properties of the TR membranes based on 6FDA drop sharply from 85.4 (250 °C) to 9.8 (475 °C) MPa. Too high thermal treatment temperature easily induces the slight pyrolysis of polymer main chain, resulting in the loss of mechanical properties. Furthermore, the porous structure caused by thermal rearrangement and crosslinking might make the polymer membrane heterogeneous, leading to the serious degradation of mechanical properties.[39]

3.5 Gas separation of PEI and TR membranes

It is well known that the gas separation properties of polymer membranes are controlled by gas solution-diffusion process. Due to the difference in the solution and diffusion coefficients of various gases in the membrane, the relative permeation rate of the gases is apparently different. Hence, the gas permeabilities of polymer membranes strongly depend on the free volume, which provides a path for the transmission of gas molecules. In view of XRD results, the as-prepared PEI and TR membranes are expected to exhibit excellent gas separation properties, so the gas permeabilities for H_2, CO_2, O_2 and N_2 are determined at 30 °C and the results are listed in Table 3. It can be seen from Table 3 that the gas permeabilities of PEI membranes are relatively low and follow the orders: $P(H_2) > P(CO_2) > P(O_2) > P(N_2)$, which is in reverse order of molecular dynamics diameter of four gases. Meanwhile, the gas permeabilities of PEI(BHAPPP-6FDA) are higher than those of other PEI membranes, which is consistent with the result of the *d*-spacing values measured by XRD and calculated FFV. Based on the same diamine, the dianhydrides take an important influence on the gas separation performance. The gas permeabilities of PEI(BHAPPP-ODPA) is comparatively low, because the flexible –O– linkage causes a dense packing of molecular segments. The

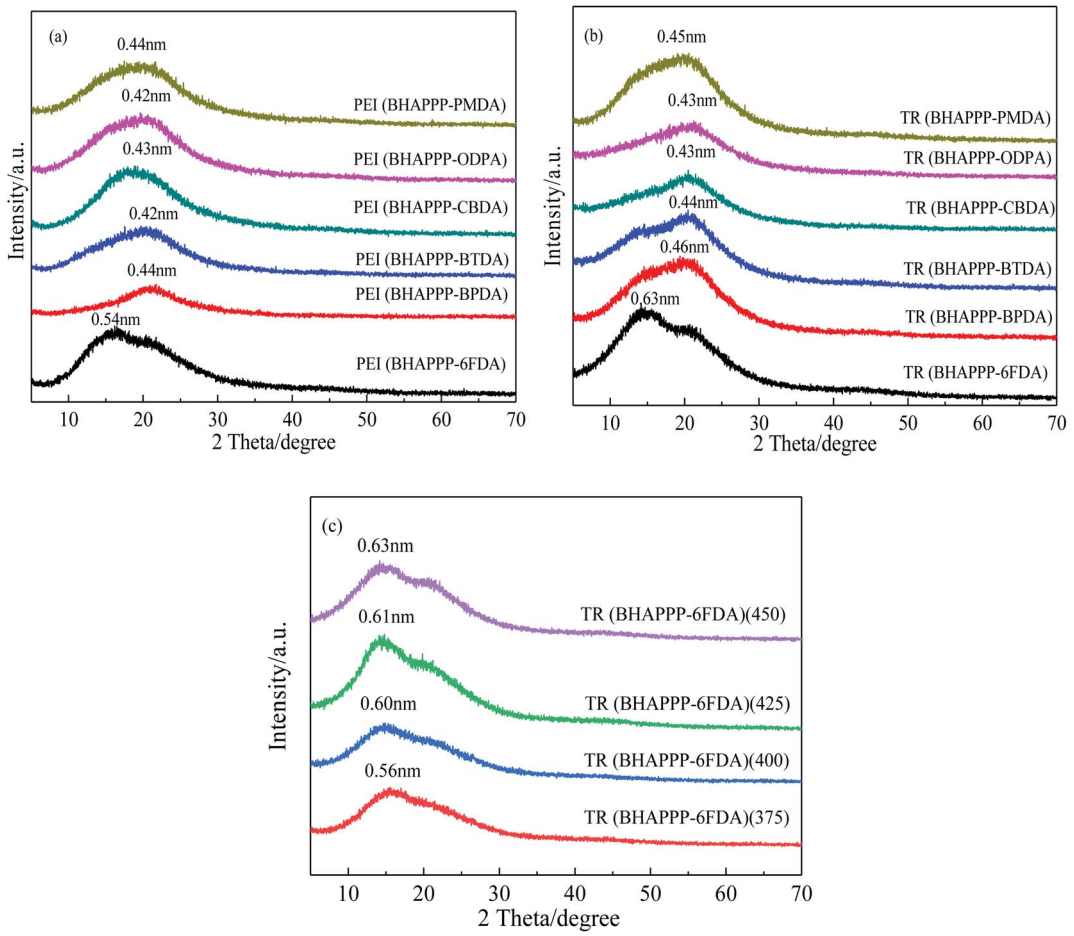

Fig. 8 XRD curves (a) PEI membranes, (b) TR membranes and (c) TR(BHAPPP-6FDA) treated at different treatment temperature.

Table 2 Physical properties of PEIs

Polymers[a]	Density (g cm^{-3})	Molar mass, M_0[b] (g mol^{-1})	Molar volume, V_0 (cm^3 mol^{-1})	van der Waals volume, V_w (cm^3 mol^{-1})	Fractional free volume, FFV[c]	d-spacing (nm)
PEI(BHAPPP-CBDA)	1.3317	764	573.7	390.1	0.116	0.43
PEI(BHAPPP-PMDA)	1.3636	688	504.5	342.3	0.118	0.44
PEI(BHAPPP-BPDA)	1.3377	764	571.1	386.6	0.120	0.44
PEI(BHAPPP-ODPA)	1.3573	780	574.7	392.1	0.114	0.42
PEI(BHAPPP-BTDA)	1.3536	792	585.1	398.3	0.115	0.42
PEI(BHAPPP-6FDA)	1.2502	914	731.1	475.1	0.156	0.54

[a] Thermally treated at 250 °C for 30 min. [b] Estimated by assuming 100% imidization conversion. [c] Fractional free volume of PEI membranes calculated by Bondi method.

PEI(BHAPPP-6FDA) shows higher gas permeabilities, which are attributed to the introduction of the large volume –C(CF$_3$)$_2$– structure. The reason for it is that the increase of interchain spacing promotes the transport of gas molecules. The gas permeabilities of PEI(BHAPPP-6FDA) reach 7.35 Barrer for CO_2, 9.25 Barrer for H_2, 1.184 Barrer for O_2, 0.249 Barrer for N_2, coupled with CO_2/N_2 of 29.51 and H_2/N_2 of 37.15. The PEI membranes containing phthalide groups exhibit no better gas permeabilities compared with some reported polymer membranes, such as PIMs and Matrimid, which is probably attributed to the dense packing of macromolecular chains caused by large amounts of hydrogen bonds because of the existence of hydroxyl groups.[60]

After thermal treatment at 450 °C for 1 h, the gas permeabilities of these TR membranes were enhanced because of the thermal rearrangement from hydroxyl-containing PEI to PBO.[34,44,59] The improvement of gas permeabilities is roughly in alignment to the XRD results. The obvious increase of d-spacing

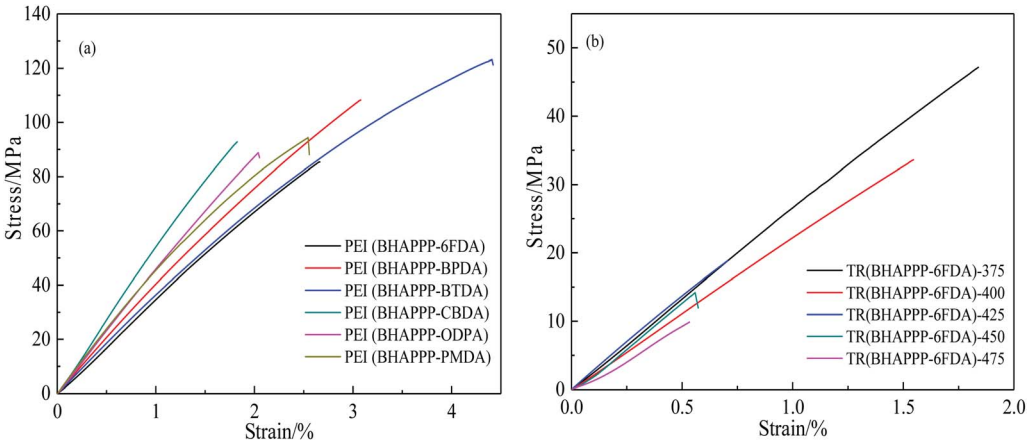

Fig. 9 Stress–strain curves (a) PEI membranes and (b) TR(BHAPPP-6FDA) membranes.

Table 3 Gas separation performance of PEI and TR membranes

	Permeability[a]/Barrer[b]				Ideal selectivity[c]		
Samples	CO_2	H_2	O_2	N_2	CO_2/N_2	O_2/N_2	H_2/N_2
PEI(BHAPPP-BPDA)	5.83	6.24	1.167	0.269	21.67	4.34	23.20
PEI(BHAPPP-BTDA)	4.67	5.43	1.224	0.241	19.45	5.10	22.53
PEI(BHAPPP-PMDA)	5.02	5.87	0.963	0.235	21.36	5.21	24.98
PEI(BHAPPP-CBDA)	2.49	3.12	0.481	0.111	22.43	4.33	28.11
PEI(BHAPPP-ODPA)	1.37	2.07	0.257	0.057	24.03	4.51	36.31
PEI(BHAPPP-6FDA)	7.35	9.25	1.184	0.249	29.51	4.75	37.15
TR(BHAPPP-BPDA)	178.96	154.97	37.86	7.39	24.21	5.12	20.97
TR(BHAPPP-BTDA)	119.23	97.05	24.00	4.56	26.14	5.26	21.28
TR(BHAPPP-PMDA)	162.11	150.60	35.41	7.24	22.39	4.89	20.80
TR(BHAPPP-CBDA)	67.98	53.13	13.98	2.72	24.99	5.13	19.53
TR(BHAPPP-ODPA)	57.77	53.86	12.06	1.87	30.89	6.45	28.80
TR(BHAPPP-6FDA)	258.5	190.5	38.35	4.25	60.82	9.02	44.82
6FDA-MPP-400 [48]	194	—	42.2	10.6	18.30	3.98	—
PEBO-6FDA[32]	245.04	272.34	60.73	10.58	23.16	5.74	25.7
6FDA-Durene/MPP[50]	219.9	689.4	66.5	24.9	8.83	2.7	25.7
6FDA-CADA1-450 [51]	1858	—	369	108	17.2	3.42	—
R-TR-PBOIa-1 h[56]	75	143	17	3.3	23	5	44

[a] All gas permeation results were obtained at 30 °C and 0.01 MPa (0.1 atm). [b] 1 Barrer = 10^{-10} cm^3 (STP)cm cm^{-2} s^{-1} cm Hg^{-1} = 3.35×10^{-16} mol m m^{-2} s^{-1} Pa^{-1}. [c] Ideal selectivities were obtained by the ratio of two gas permeabilities.

of TR(BHAPPP-6FDA) indicates that the conversion rate of thermal rearrangement is relatively high, forming more free volume to readily transport the gas molecules. Among them, the TR(BHAPPP-6FDA) shows higher gas permeabilities and excellent selectivities, including CO_2 of 258.5 Barrer, H_2 of 190.5 Barrer, O_2 of 38.35 Barrer, N_2 of 4.25 Barrer and CH_4 of 2.15 Barrer, coupled with CO_2/CH_4 of 120.2 and O_2/N_2 of 9.02. Compared with the PEBO-6FDA membrane containing fluorene groups reported by our group, the as-prepared TR(BHAPPP-6FDA) exhibit extremely higher gas selectivities, which is mostly assigned to the thermal crosslinking of phthalide groups.[32]

In addition, compared with 6FDA-MPP-400[48] and 6FDA-Durene/MPP[50] containing phthalide structure, the TR(BHAPPP-6FDA) displays higher gas permeabilities. However, compared with 6FDA-CADA1-450 with a carboxyl group from the ring-opening of phthalide structure,[51] the gas permeabilities are obviously lower. This may be due to the fact that the phthalide groups of TR(BHAPPP-6FDA) don't completely open ring and decarboxylate, and the cross-linking process is relatively limited in the TR process. For polymer membranes, the gas separation mainly follows to the solution-diffusion mechanism.[12] With the occurrence of TR and crosslinking reaction, a large number of porous and network structures are formed, resulting in sieving separation.[47] Meanwhile, the formation of crosslinking structure enhances the interaction between macromolecular chains and forms rigid networks, which greatly contributes to the increase of gas selectivities. The possible crosslinking model is shown in Fig. 10, in which the biphenyl crosslinking structure is formed between adjacent phenyl radicals according to the literature.[47] Furthermore, it is observed from Table 3 that the permeability of CO_2 for TR membranes exceeds that of H_2,

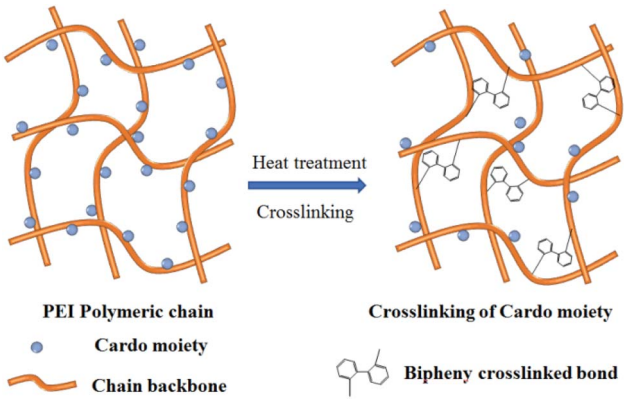

Fig. 10 Crosslinking model of phthalide Cardo moiety during TR process.

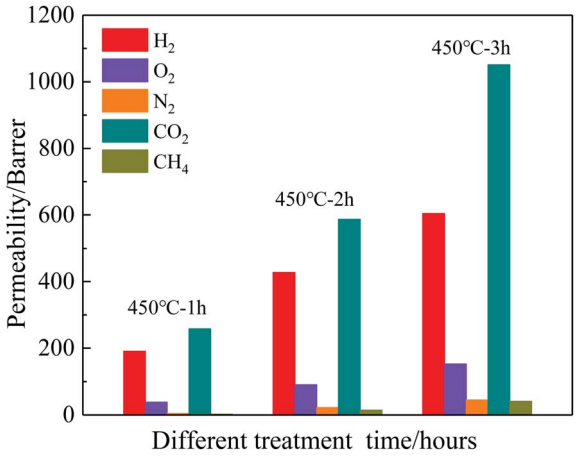

Fig. 12 Gas permeabilities of TR(BHAPPP-6FDA) membranes treated at 450 °C with different time.

indicating the better solubility of CO_2 in the TR matrix. As a result, the gas permeabilities of these TR membrane materials are significantly increased after thermal rearrangement, while the selectivities are also increased in varying degrees or declined slightly, which overcome the trade-off relationship in some sense.

Selected the TR(BHAPPP-6FDA) sample as target, the effects of thermally treated temperature and time on the gas permeabilities are also investigated, and the obtained data are illustrated in Fig. 11 and 12, respectively. With the increase of thermally treated temperature and time, the degree of thermally rearranged reaction gradually increase, resulting in the more release of CO_2. It can be found that the four gas permeabilities of TR membranes extremely increase with the increase of temperature, but too high temperature will lead to the pyrolysis reaction instead of the rearrangement reaction. Thus, within the temperature range of TR, the structure conversion is partially completed and the gas permeabilities are improved significantly. Besides, CH_4 gas was also used to test the gas permeabilities of TR(BHAPPP-6FDA)-450 membrane with different treatment time. With the extension of thermal processing time, the permeabilities of five gases are greatly increased. When the thermal rearrangement time is 3 h, the permeabilities of H_2, CO_2, O_2, N_2 and CH_4 separately reach 604, 1051, 152, 45 and 41 Barrers, but the selectivity of O_2/N_2 drops from 8.97 to 3.38 and CO_2/CH_4 decreases from 120.97 to 25.63. Hence, the thermal treatment temperature and time play a key role on the gas separation performance.

In order to investigate the effect of test pressure, the gas permeability test of TR(BHAPPP-6FDA) membrane was carried out at 0.1, 0.5 and 1.0 atm, respectively. Because the tested membrane sample was unsupported, too high pressure wasn't adopted to avoid rupture of the membranes. Fig. 13 gives the gas permeabilities at different pressures, and it can be seen that the permeabilities of four gases exhibit a slight downward trend as the pressure gradually increases. Among them, the permeability of CO_2 is obviously affected by test pressure due to the decrease of gas adsorption or dissolution in membrane materials. This behavior is typical for glassy polymers.[61]

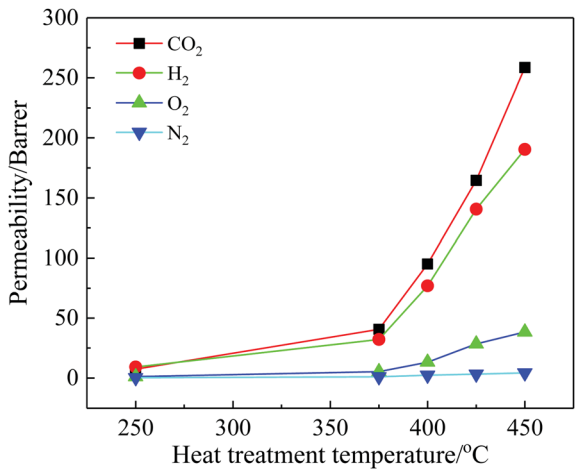

Fig. 11 Gas permeabilities of TR(BHAPPP-6FDA) membranes treated at different temperatures.

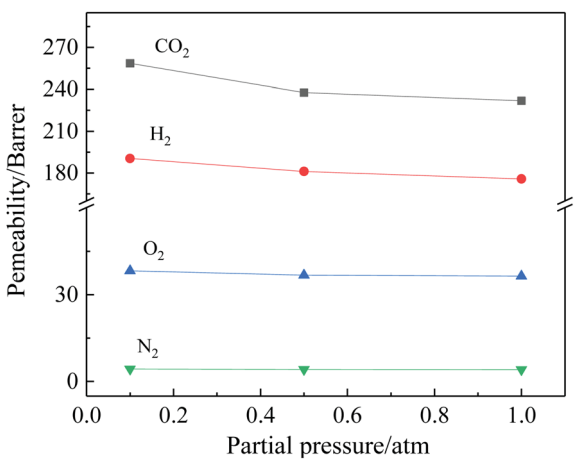

Fig. 13 Gas permeabilities of TR(BHAPPP-6FDA) membrane at different test pressure.

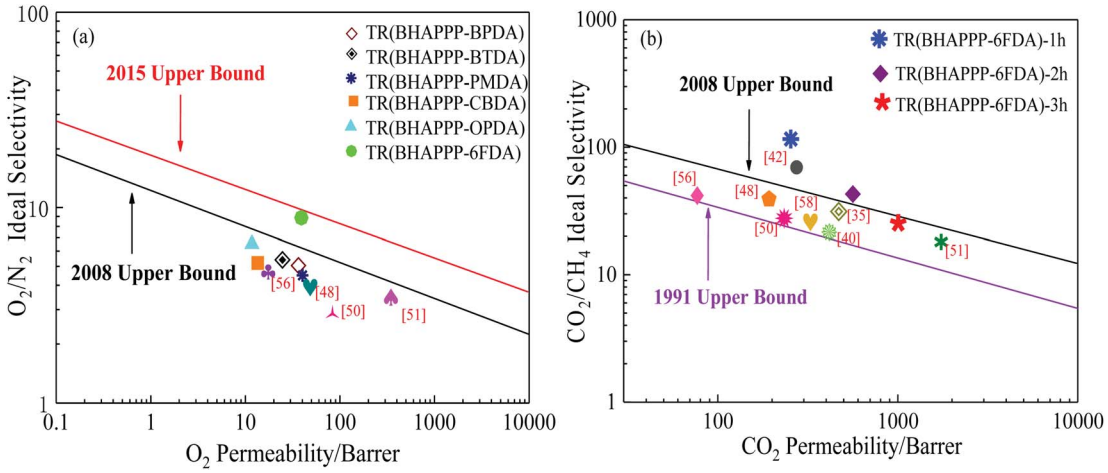

Fig. 14 Evaluation of separation performance of TR membranes (a) O_2 *vs.* O_2/N_2; (b) CO_2 *vs.* CO_2/CH_4.

In gas separation application, the "trade-off" relationship between permeability and selectivity constantly exists, resulting in any improvement in gas permeability accompanied with a decrease of selectivity. The O_2/N_2 and CO_2/CH_4 separation properties of TR membranes in this work and many reported TR membranes are depicted in Fig. 14. Compared with aPBO,[58] R-TR-PBOIa-1 h,[56] PEBO-6FDA,[32] 6FDA-MPP-400,[48] 6FDA-CADA1-450,[51] and 6FDA-Durene/MPP,[50] the TR(BHAPPP-6FDA) membrane exhibits the best O_2/N_2 separation properties, close to the 2015 upper limit. Moreover, the CO_2/CH_4 separation properties of TR(BHAPPP-6FDA) show a decline trend with the lapse of thermal treatment time, but the TR(BHAPPP-6FDA)-1 h still greatly exceeds the 2008 upper limit. Thus, among the six TR membranes, the TR(BHAPPP-6FDA) membrane displays superior gas separation performance due to the larger *d*-spacing caused by $-C(CF_3)_2-$ structures, which is expected to be applied as separation materials in the future.

4. Conclusions

The diamines 3,3-bis[4-(3-hydroxy-4-aminophenoxy)phenyl] phthalide (BHAPPP) were successfully synthesized and polymerized with six kinds of dianhydrides to prepare PEI membranes. Then, the corresponding TR membranes were obtained by thermal treatment at 450 °C for 1 h. The PEI membranes showed excellent mechanical properties, such as tensile strength of 85.4–122.9 MPa and Young's modulus of 3.3–5.1 GPa. However, as the thermal treatment temperature increased, the mechanical properties of the membranes sharply decreased. Meanwhile, the gas permeabilities were greatly increased because of the thermal rearrangement from hydroxyl-containing PEI to TR membranes. Particularly, during the thermal rearrangement, the thermal crosslinking reaction derived from phthalide groups took place simultaneously, resulting in the obvious improvement in gas selectivities than similar structure TR membranes containing fluorenyl structures. Importantly, the treatment temperature and time played a major role in gas separation performance of TR membranes. Comparatively, the gas permeabilities of TR(BHAPPP-6FDA) for CO_2, H_2, O_2, N_2 and CH_4 reached 258.5, 190.5, 38.35, 4.25 and 2.15 Barrers, respectively. The selectivity for O_2/N_2 was 9.02, close to the 2015 Robeson upper limit, and CO_2/CH_4 reached 120.2, which significantly exceeded the 2008 Robeson upper limit. Therefore, this work provides a kind of TR membranes based on phthalide groups with excellent gas separation properties, which are expected to be used as gas separation materials in the practical application.

Conflicts of interest

There are no conflicts to declare.

Acknowledgements

The work was financially supported by National Natural Science Foundation of China Grants (contract grant number: 21878033) and the Talent Project of Liaoning University of Science and Technology (No. 601011507-17).

References

1 J. Gao, H. Mao, H. Jin, C. Chen, A. Feldhoff and Y. Li, Functionalized ZIF-7/Pebax® 2533 mixed matrix membranes for CO2/N2 separation, *Microporous Mesoporous Mater.*, 2020, **297**, 110030.
2 Y. Xiao, B. T. Low, S. S. Hosseini, T. S. Chung and D. R. Paul, The strategies of molecular architecture and modification of polyimide-based membranes for CO2 removal from natural gas-A review, *Prog. Polym. Sci.*, 2009, **34**, 561–580.
3 A. L. Ahmad, Z. A. Jawad, S. C. Low and S. H. S. Zein, A cellulose acetate/multi-walled carbon nanotube mixed matrix membrane for CO2/N2 separation, *J. Membr. Sci.*, 2014, **451**, 55–66.
4 Z. Wang, D. Wang and J. Jin, Microporous polyimides with rationally designed chain structure achieving high

performance for gas separation, *Macromolecules*, 2014, **47**, 7477–7483.

5 S. A. Stern, Y. Mi, H. Yamamoto and A. K. S. Clair, Structure/permeability relationships of polyimide membranes. Applications to the separation of gas mixtures, *J. Polym. Sci., Part B: Polym. Phys.*, 1989, **27**, 1887–1909.

6 V. M. Magueijo, L. G. Anderson, A. J. Fletcher and S. J. Shilton, Polysulfone mixed matrix gas separation hollow fiber membranes filled with polymer and carbon xerogels, *Chem. Eng. Sci.*, 2013, **92**, 13–20.

7 C. L. Aitken, W. J. Koros and D. R. Paul, Effect of structural symmetry on gas transport properties of polysulfones, *Macromolecules*, 1992, **25**, 3424–3434.

8 L. M. Robeson, Correlation of separation factor *versus* permeability for polymeric membranes, *J. Membr. Sci.*, 1991, **62**, 165–186.

9 L. M. Robeson, The upper bound revisited, *J. Membr. Sci.*, 2008, **320**, 390–400.

10 R. Swaidan, B. Ghanem and I. Pinnau, Fine-tuned intrinsically ultramicroporous polymers redefine the permeability/selectivity upper bounds of membrane-based air and hydrogen separations, *ACS Macro Lett.*, 2015, **4**, 947–951.

11 W. H. Lee, J. G. Seong, X. F. Hu and Y. M. Lee, Recent progress in microporous polymers from thermally rearranged polymers and polymers of intrinsic microporosity for membrane gas separation: Pushing performance limits and revisiting trade-off lines, *J. Polym. Sci.*, 2020, **58**, 2450–2466.

12 Y. H. Yang, J. C. Xia, Z. J. Ding, Y. X. Zheng, S. J. Ding and Y. Z. Shen, Synthesis and resistive switching characteristics of polyimides derived from 2,7-aryl substituents tetraphenyl fluorene diamines, *Eur. Polym. J.*, 2018, **108**, 85–97.

13 C. Y. Park, E. H. Kim, J. H. Kim, Y. M. Lee and J. H. Kim, Novel semi-alicyclic polyimide membranes:Synthesis, characterization, and gas separation properties, *Polym. J.*, 2018, **151**, 325–333.

14 Y. B. Zhuang, J. G. Seong and Y. M. Lee, Polyimides containing aliphatic/alicyclic segments in the main chains, *Prog. Polym. Sci.*, 2019, **92**, 35–88.

15 S. L. Wang, S. Z. Jin, X. C. Han, L. Li, X. G. Zhao, H. W. Zhou and C. H. Chen, Insights into the relationship between structure and properties of Spirobichroman-based polyimides: Effects of substituents on molecular structure and gas separation, *Mater. Des.*, 2020, **9**, 108933.

16 T. Y. Li, J. J. Liu, S. S. Zhao, Z. Q. Chen, H. H. Huang, R. L. Guo and Y. M. Chen, Microporous polyimides containing bulky tetra-o-isopropyl and naphthalene groups for gas separation membranes, *J. Membr. Sci.*, 2019, **585**, 282–288.

17 N. Alaslai, B. Ghanem, F. Alghunaimi and I. Pinnau, High-performance intrinsically microporous dihydroxyl-functionalized triptycene-based polyimide for natural gas separation, *Polymer*, 2016, **91**, 128–135.

18 G. Chen, X. S. Zhang, S. B. Zhang, T. L. Chen and Y. L. Wu, Synthesis, properties, and gas permeation performance of cardo poly(arylene ether sulfone)s containing phthalimide side groups, *J. Appl. Polym. Sci.*, 2007, **106**, 2808–2816.

19 G. X. Deng, Y. L. Wang, X. P. Zong, X. X. Yuan, J. Z. Luo, X. Z. Wang and S. Xue, Gas transport property of the binaphthyl-based polyimide membranes, *Polymer*, 2019, **183**, 121854.

20 W. Dujardin, C. V. Goethem, Z. D. Zhang, R. Verbeke, M. Dickmann, W. Egger, E. Nies, L. Vankelecom and G. Koeckelberghs, Fine-tuning the molecular structure of binaphthalene polyimides for gas separations, *Eur. Polym. J.*, 2019, **114**, 134–143.

21 X. F. Hu, W. H. Lee, J. Y. Zhao, J. Y. Ba, J. S. Kim, Z. Wang, J. L. Yan, Y. B. Zhuang and Y. M. Lee, Troger's Base (TB)-containing polyimide membranes derived from bio-based dianhydrides for gas separations, *J. Membr. Sci.*, 2020, **610**, 118255.

22 S. J. Luo, Q. N. Zhang, T. K. Bear, T. E. Curtis, R. K. Roeder, C. M. Doherty, A. J. Hillc and R. L. Guo, Triptycene-containing poly(benzoxazole-co-imide) membranes with enhanced mechanical strength for high-performance gas separation, *J. Membr. Sci.*, 2018, **551**, 305–314.

23 B. B. Shrestha, K. Wakimoto, Z. G. Wang, A. P. Isfahani, T. Suma, E. Sivaniah and B. Ghalei, A facile synthesis of contorted spirobisindane-diamine and its microporous polyimides for gas separation, *RSC Adv.*, 2018, **12**, 6326–6330.

24 Z. G. Wang, D. Wang, F. Zhang and J. Jin, Troger's base-based microporous polyimide membranes for high-performance gas separation, *ACS Macro Lett.*, 2014, **3**, 597–601.

25 Q. N. Zhang, S. J. Luo, J. R. Weidman and R. L. Guo, Preparation and gas separation performance of mixed-matrix membranes based on triptycene-containing polyimide and zeolite imidazole framework (ZIF-90), *Polymer*, 2017, **131**, 209–216.

26 J. G. Seong, Y. B. Zhuang, S. J. Kim, Y. S. Do, W. H. Lee, M. Guiverc and Y. M. Lee, Effect of methanol treatment on gas sorption and transport behavior of intrinsically microporous polyimide membranes incorporating Tröger's base, *J. Membr. Sci.*, 2015, **480**, 104–114.

27 Y. Zhang, W. H. Lee, J. G. Seong, J. Y. Bae, Y. B. Zhuang, S. C. Feng, Y. H. Wan and Y. M. Lee, Alicyclic segments upgrade hydrogen separation performance of intrinsically microporous polyimide membranes, *J. Membr. Sci.*, 2020, **611**, 118363.

28 Y. B. Zhuang, J. G. Seong, Y. S. Do, W. H. Lee, M. J. Lee, M. Guiver and Y. M. Lee, High-strength, soluble polyimide membranes incorporating Tröger's base for gas separation, *J. Membr. Sci.*, 2016, **504**, 55–65.

29 B. Comesaña-Gandara, L. Ansalonic, Y. M. Lee, A. E. Lozano and M. G. De Angelis, Sorption, diffusion, and permeability of humid gases and aging of thermally rearranged (TR) polymer membranes from a novel ortho-hydroxypolyimide, *J. Membr. Sci.*, 2017, **542**, 439–455.

30 A. Brunettia, E. Toccia, M. Cersosimoa, J. S. Kim, W. H. Lee, J. G. Seong, Y. M. Lee, E. Driolia and G. Barbieri, Mutual influence of mixed-gas permeation in thermally rearranged

poly(benzoxazole-co-imide) polymer membranes, *J. Membr. Sci.*, 2019, **580**, 202–213.

31 J. S. Kim, S. J. Moon, H. H. Wang, S. J. Kim and Y. M. Lee, Mixed matrix membranes with a thermally rearranged polymer and ZIF-8 for hydrogen separation, *J. Membr. Sci.*, 2019, **582**, 381–390.

32 Y. H. Lu, J. H. Zhang, G. Y. Xiao, L. Li, M. J. Hou, J. Y. Hu and T. H. Wang, Synthesis and gas permeation properties of thermally rearranged poly(ether-benzoxazole)s with low rearrangement temperatures, *RSC Adv.*, 2020, **10**, 17461–17472.

33 S. J. D. Smith, R. J. Hou, C. H. Lau, K. Konstas, M. Kitchin, G. X. Dong, J. Lee, W. H. Lee, J. G. Seong, Y. M. Lee and M. R. Hill, Highly permeable thermally rearranged mixed matrix membranes (TR-MMM), *J. Membr. Sci.*, 2019, **585**, 260–270.

34 W. H. Lee, J. G. Seong, J. Y. Bae, H. H. Wang, S. J. Moon, J. T. Jung, Y. S. Do, H. Kang, C. H. Park and Y. M. Lee, Thermally rearranged semi-interpenetrating polymer network (TR-SIPN) membranes for gas and olefin/paraffin separation, *J. Membr. Sci.*, 2021, **625**, 119157.

35 M. Calle and Y. M. Lee, Thermally rearranged (TR) poly(ether-benzoxazole) membranes for gas separation, *Macromolecules*, 2011, **44**, 1156–1165.

36 S. Bandehali, A. E. Amooghin, H. Sanaeepur, R. Ahmadi, A. Fuoco, J. C. Jansen and S. Shirazian, Polymers of intrinsic microporosity and thermally rearranged polymer membranes for highly efficient gas separation, *Sep. Purif. Technol.*, 2021, **278**, 119513.

37 J. H. Zhang, Y. H. Lu, G. Y. Xiao, M. J. Hou, L. Li and T. H. Wang, Enhanced gas separation and mechanical properties of fluorene-based thermal rearrangement copolymers, *RSC Adv.*, 2021, **11**, 13164–13174.

38 X. F. Hu, W. H. Lee, J. Y. Zhao, J. S. Kim, Z. Wang, J. Yan, Y. B. Zhuang and Y. M. Lee, Thermally rearranged polymer membranes containing highly rigid biphenyl ortho-hydroxyl diamine for hydrogen separation, *J. Membr. Sci.*, 2020, **604**, 118053.

39 J. Kostina, O. Rusakova, G. Bondarenko, A. Alentiev, T. Meleshko, N. Kukarkina, A. Yakimanskii and Y. Yampolskii, Thermal rearrangement of functionalized polyimides: IR-spectral, quantum chemical studies and gas permeability of TR polymers, *Ind. Eng. Chem. Res.*, 2013, **52**, 10476–10483.

40 L. Ye, X. M. Jie, L. Wang, G. H. Xu, Y. Sun, G. D. Kang and Y. M. Cao, Preparation and gas separation performance of thermally rearranged poly (benzoxazole-co-amide) (TR-PBOA) hollow fiber membranes deriving from polyamides, *Sep. Purif. Technol.*, 2021, **257**, 117870.

41 C. Aguilar-Lugo, W. H. Lee, J. Miguel, J. Campa, P. Prádanos, J. Y. Bae, Y. M. Lee, C. Álvarez and Á. Lozano, Highly permeable mixed matrix membranes of thermally rearranged polymers and porous polymer networks for gas separations, *ACS Appl. Polym. Mater.*, 2021, **3**, 5224–5235.

42 S. J. Luo, J. Y. Liu, H. Q. Lin, B. A. Kazanowska, M. D. Hunckler, R. K. Roeder and R. L. Guo, Preparation and gas transport properties of triptycene-containing polybenzoxazole (PBO)-based polymers derived from thermal rearrangement (TR) and thermal cyclodehydration (TC) processes, *J. Mater. Chem. A*, 2016, **4**, 17050–17062.

43 S. Luo, Q. Zhang, T. K. Bear, T. E. Curtis, R. K. Roeder, C. M. Doherty, A. J. Hill and R. Guo, Triptycene-containing poly(benzoxazole-co-imide) membranes with enhanced mechanical strength for high-performance gas separation, *J. Membr. Sci.*, 2018, **551**, 305–314.

44 Z. P. Smith, D. F. Sanders, C. P. Ribeiro, R. Guo, B. D. Freeman, D. R. Paul, J. E. McGrath and S. Swinnea, Gas sorption and characterization of thermally rearranged polyimides based on 3,3'-dihydroxy-4,4'-diamino-biphenyl (HAB) and 2,2'-bis-(3,4-dicarboxyphenyl) hexafluoropropane dianhydride (6FDA), *J. Membr. Sci.*, 2012, **415–416**, 558–567.

45 M. Balçık, S. Velioglu, S. B. Tantekin-Ersolmaz and M. G. Ahunbay, Can crosslinking improve both CO2 permeability and plasticization resistance in 6FDA-pBAPS/DABA copolyimides?, *Polymer*, 2020, **205**, 122789.

46 H. An, A. S. Lee, I. Kammakakam, S. S. Hwang, J. H. Kim, J. H. Lee and J. S. Lee, Bromination/Debromination-induced thermal crosslinking of 6FDA-Durene for aggressive gas separations, *J. Membr. Sci.*, 2018, **545**, 358–366.

47 R. S. Xu, L. Li, X. Jin, M. J. Hou, L. He, Y. H. Lu, C. W. Song and T. H. Wang, Thermal crosslinking of a novel membrane derived from phenolphthaleinbased cardo poly(arylene ether ketone) to enhance CO2/CH4 separation performance and plasticization resistance, *J. Membr. Sci.*, 2019, **586**, 306–317.

48 C. L. Zhang, B. Cao and P. Li, Thermal oxidative crosslinking of phenolphthalein-based cardo polyimides with enhanced gas permeability and selectivity, *J. Membr. Sci.*, 2018, **546**, 90–99.

49 Z. K. Tian, B. Cao and P. Li, Effects of sub-Tg cross-linking of triptycene-based polyimides on gas permeation, plasticization resistance and physical aging properties, *J. Membr. Sci.*, 2018, **560**, 87–96.

50 L. M. Deng, Y. L. Xue, J. Yan, C. H. Lau, B. Cao and P. Li, Oxidative crosslinking of copolyimides at sub-Tg temperatures to enhance resistance against CO2-induced plasticization, *J. Membr. Sci.*, 2019, **583**, 40–48.

51 C. L. Zhang, P. Li and B. Cao, Decarboxylation crosslinking of polyimides with high CO2/CH4 separationperformance and plasticization resistance, *J. Membr. Sci.*, 2017, **528**, 206–216.

52 M. Calle, H. J. Jo, C. M. Doherty, A. J. Hill and Y. M. Lee, Cross-Linked thermally rearranged poly(benzoxazole-co-imide) membranes prepared from ortho-Hydroxycopolyimides containing pendant carboxyl groups and gas separation properties, *Macromolecules*, 2015, **48**, 2603–2613.

53 K. Cao, M. X. Zhang and G. L. Liu, The effect of end group and molecular weight on the yellowness of polyetherimide, *Macromol. Rapid Commun.*, 2018, **39**, 1800045.

54 J. S. Kang, J. Won, H. C. Park, U. Y. Kim, Y. S. Kang and Y. M. Lee, Morphology control of asymmetric membranes

by UV irradiation on polyimide dope solution, *J. Membr. Sci.*, 2000, **169**, 229–235.

55 D. M. Knauss and J. T. Bender, Phthalide as an activating group for the synthesis of poly(aryl ether phthalide)s by nucleophilic aromatic substitution, *J. Polym. Sci., Part A: Polym. Chem.*, 2002, **40**, 3046–3054.

56 Y. B. Zhuang, J. G. Seong, W. H. Lee, Y. S. Do, M. J. Lee, G. Wang, M. Guiver and Y. M. Lee, Mechanically tough, thermally rearranged (TR) random/block poly(benzoxazole-co-imide) gas separation membranes, *Macromolecules*, 2015, **48**, 5286–5299.

57 Y. S. Do, W. H. Lee, J. G. Seong, J. S. Kim, H. H. Wang, C. Doherty, A. Hill and Y. M. Lee, Thermally rearranged (TR) bismaleimide-based network polymers for gas separation membranes, *Chem. Commun.*, 2016, **52**, 13556–13559.

58 W. H. Lee, J. G. Seong, J. Y. Bae, H. H. Wang, S. J. Moon, J. T. Jung, Y. S. Do, H. Kang, C. H. Park and Y. M. Lee, Thermally rearranged semi-interpenetrating polymer network (TR-SIPN) membranes for gas and olefin/paraffin separation, *J. Membr. Sci.*, 2021, **625**, 119157.

59 Y. B. Zhuang, J. G. Seong, Y. S. Do, H. J. Jo, M. J. Lee, G. Wang, M. Guiver and Y. M. Lee, Effect of isomerism on molecular packing and gas transport properties of poly(benzoxazole-co-imide)s, *Macromolecules*, 2014, **47**, 7947–7957.

60 H. Shamsipur, B. A. Dawood, P. M. Budd, P. Bernardo, G. Clarizia and J. C. Jansen, Thermally rearrangeable PIM-polyimides for gas separation membranes, *Macromolecules*, 2014, **47**, 5595–5606.

61 W. J. Koros, A. H. Chan and D. R. Paul, Sorption and transport of various gases in polycarbonate, *J. Membr. Sci.*, 1977, **2**, 165–190.